

# Comparison of chain versus sheet crystal structures for cyanides $MCN$ ( $M = \text{Cu-Au}$ ) and dicarbides $MC_2$ ( $M = \text{Be-Ba; Zn-Hg}$ ). Alternatives to graphene ?

P. Zaleski-Ejgierd and P. Pyykkö

Laboratory for Instruction in Swedish, Department of Chemistry,  
P.O.B. 55, FIN-00014 University of Helsinki, Finland

M. Hakala

Division of X-ray Physics, Department of Physical Sciences,  
P.O.B. 64, FIN-00014 University of Helsinki, Finland

(Dated: May 9, 2018)

The cyanides  $MCN$ ,  $M=\text{Cu, Ag, Au}$ , have experimentally a structure with hexagonally packed, infinite  $-M-CN-M-CN-$  chains. Following our earlier study for  $\text{AuCN}$ , we now predict that all three  $MCN$  could have an alternative  $M_3C_3N_3$  sheet structure of comparable energy with the known one. The valence isoelectronic systems  $MC_2$  versus  $M_3C_6$ ,  $M=\text{Be-Ba; Zn-Hg}$  are also studied. Now, the known dicarbides have the  $\text{CaC}_2$  or  $\text{MgC}_2$  chain structures. The predicted sheets lie energetically below the chains for  $M = \text{Zn, Cd, and Hg}$ . All these systems are experimentally unknown. Indeed, they are clearly endothermic, compared to the elements. For some sheet structures the densities of states suggests rather small band gaps and even metallic character. When available, the experimental geometries agree well with the calculated ones for both cyanides and dicarbides.

## I. INTRODUCTION

One of the fundamental goals of computational quantum chemistry is the prediction of new chemical species and the determination of their properties<sup>1</sup>. A recent example is gold cyanide,  $\text{AuCN}$ , a well-known commodity chemical, whose known structure consists of infinite  $-\text{CN-Au-CN-Au}-$  chains<sup>2</sup>. The chains are packed together on a hexagonal grid in such a way, that the Au atoms are in the same plane (see Fig. 1: A'). However, Hakala and Pyykkö<sup>3</sup> recently predicted for  $\text{AuCN}$  an alternative crystal structure, having a closely similar energy but only  $\sim 70\%$  of the density (see Fig. 1: B'). The new structure contains triazine-type six-rings of three carbon and three nitrogen atoms,  $\text{C}_3\text{N}_3$ , which are coupled to each other by linearly coordinated gold(I) atoms forming a two-dimensional sheet structure. The sheets attract each other weakly due to the gold-gold aurophilic interaction. Such a new structure has not yet been observed. Since single-sheet-type 2D atomic crystals, like graphene, are potentially a very important class of materials but much less known than the 3D counterparts<sup>4</sup>, it is interesting to ask whether such a structure could also be found for other similar systems, such as the cyanides involving the other Group 11 (coinage) metals, namely copper and silver. Their known crystalline structure is also chain-type:  $-\text{CN-M-CN-M}-$  ( $M$  denoting the metal)<sup>5,6,7</sup>.

By applying the valence isoelectronic principle, one can extend the search for such a new sheet-type structures to further cases. Replacing the formula  $MCN$  of the metal cyanides by the formula  $MC_2$ , with an  $(ns)^2$  configuration for the neutral metal atom  $M$ , leads to the class of crystalline dicarbides. Metallic dicarbides may have interesting electronic properties, such as the

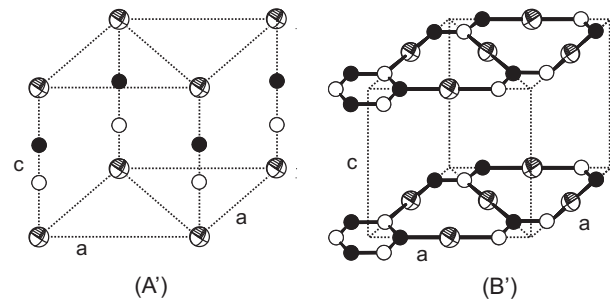


FIG. 1: Investigated crystal structures for Group 11 metal cyanides ( $M$ : spheres, C: black circles, N: white circles): A' - chain structure  $MCN$  ( $P6mm$ ), B' - sheet structure  $M_3C_3N_3$  ( $P62m$ ).

superconductivity of  $\text{YC}_2$  and its layered compounds<sup>8</sup>. In the present work we have studied metallic elements in Groups 2 (alkaline earth metals  $M=\text{Be, Mg, Ca, Sr, Ba}$ ), and 12 (transition metals  $M=\text{Zn, Cd and Hg}$ ). Stable crystalline structures are known only for some of these systems ( $\text{MgC}_2$ ,  $\text{CaC}_2$ ,  $\text{SrC}_2$ ,  $\text{BaC}_2$ ). No earlier data were found for any Group 12 dicarbides. The previously known crystal structures of  $\text{CaC}_2$ ,  $\text{SrC}_2$ ,  $\text{BaC}_2$  from Group 2 consist of infinite  $-M-CC-M-CC-$  chains, but each cation is now equatorially surrounded by four anions, each parallel to the  $z$  axis (see Fig. 2: B). Another known Group 2 dicarbide,  $\text{MgC}_2$ , also has infinite chains, but the four equatorial dicarbide ligands around the cation are now perpendicular to the  $z$  axis (see Fig. 2: C). These structures have been only very recently clarified by X-ray and neutron diffraction<sup>9,10,11</sup>.

In the present work we show that sheet-type structures such as the poly(triaurotriazine), one recently reported<sup>3</sup>

for AuCN can be also found for the other Group 11 coinage metal cyanides and for the Group 2 and 12 dicarbides. All the proposed sheet structures seem to be entirely new. For Group 12 dicarbides and for BeC<sub>2</sub> of Group 2 we also investigate whether they could form stable structures in the tetragonal geometry starting the search from the experimental geometry known for Group 2. We have performed density of states (DOS) analysis for both isolated and packed structures, and discuss the insulator vs. metallic properties of the studied systems. Vibrational analysis has been performed to provide tools for the identification and to analyze the stability of the systems. The geometries and frequencies are compared to the known cyanide and dicarbide results. Finally, the thermodynamical preferences of the predicted dicarbides are estimated by calculating their formation energies with respect to the elemental metals and graphite as starting materials.

## II. METHOD

All calculations were performed within density functional theory (DFT), using the Vienna *ab-initio* Simulation Package<sup>12,13,14</sup> (VASP). Plane-wave basis sets, Ultrasoft (US) pseudopotentials<sup>15,16</sup> and projector augmented-wave (PAW) potentials<sup>17,18</sup> with the generalized gradient approximation<sup>19</sup> (GGA) for the Perdew-Burke-Ernzerhof<sup>20</sup> (PBE) exchange-correlation functional, were employed. When optimizing the lattice parameters and the atomic positions, constant-volume calculations were performed with the symmetry of the unit cell kept fixed. We typically scanned the crystal volume for each system by changing the interchain or intersheet distance in steps of 0.1 Å and letting the system relax. In this work we will report the energy value and the atomic geometry corresponding to the minimum point on the total energy curve for each system.

For the energy cutoff we used a standard 400 eV value. A  $\Gamma$ -centered  $6 \times 6 \times 6$  k-point grid was used throughout the work for the lattice optimizations and vibrational analysis. All the chain structures and the majority of the sheet structures studied were found to be insulators, and this choice of the k-point grid was found sufficient for the convergence in total energy and geometry. For the dynamical matrix and vibrational frequencies a shift of 0.025 Å was applied to the atomic positions. Some sheet structures exhibited the closing of the band gap as the sheets were packed together, and two dicarbides were manifestly metallic already as isolated sheets. The semimetallic vs. metallic character for these systems was inferred by studying the DOS at the Fermi level. For the systems with a small band gap the used k-point grid may lead to a slight overestimation of the total energy ( $\sim 0.005$  eV) and the sheet-sheet distance ( $\sim 0.2$  Å), as compared with the calculations using denser k-point grids. We expect a similar behavior also for the two metallic systems. In our tests, the intrachain and intrasheet dis-

tances C-N, M-C and M-N were well converged within 0.2% with respect to increasing the k-point grid above that of  $6 \times 6 \times 6$ . When the dispersion interactions are the dominant mechanism, such as in the case of interchain distances in cyanides, the present DFT-GGA results are not expected to be reliable and should be considered with caution.

The studied geometries are illustrated in Figs. 1-4. We refer to the geometries as 'chains' (see Fig. 1: A' and Fig. 2: A, B, C), and to the rest as 'sheets'. Furthermore, it turned out to be necessary to consider four different packings of the sheets: 'Simple stacking', where each 2D 'sheet' is simply repeated in the perpendicular direction to form the 3D crystal (see Fig. 1: B' and Fig. 3: D); 'Shifted', where every second 2D sheet is parallelly displaced, so that the benzene-like carbon ring lies on top of the 'triangle' formed by the metal atoms (see Fig. 3: E); 'Rotated', as 'simple stacking', but the carbon ring is rotated inside the sheet with respect to the connecting metals by 30° (see Fig. 4: F); 'Shifted+rotated', where in addition to the 'rotated' structure, there is also the displacement parallel to the plane as described above (see Fig. 4: G).

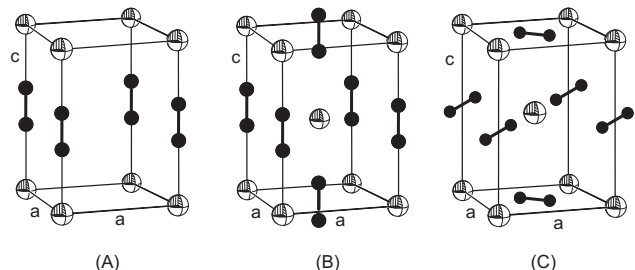


FIG. 2: Investigated crystal structures for chain-type metal dicarbides  $MC_2$  ( $M$ : spheres,  $C$ : black circles): A - tetragonal ( $P4/mmm$ ), B - tetragonal ( $I4/mmm$ ), C - tetragonal ( $I4_2/mnm$ ).

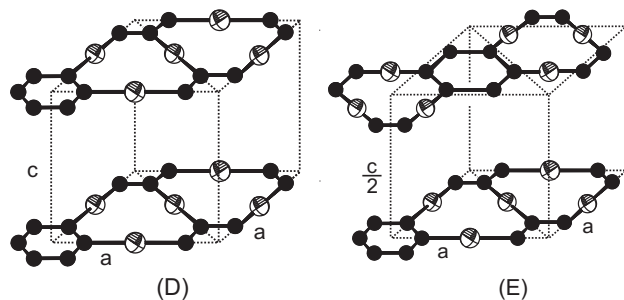


FIG. 3: Investigated crystal structures for sheet-type metal dicarbides  $M_3C_6$  ( $M$ : spheres,  $C$ : black circles): D - simple stacking ( $P\frac{6}{m}mm$ ), E - shifted ( $P6_2m$ ).

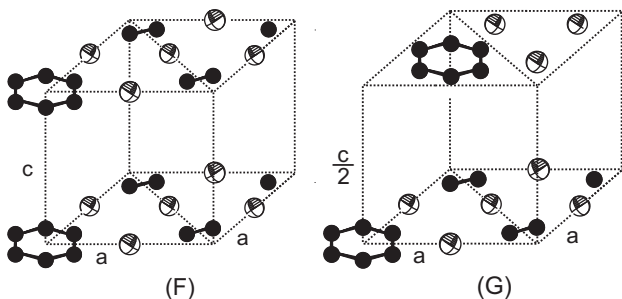


FIG. 4: Investigated crystal structures for sheet-type metal dicarbides  $M_3C_6$  ( $M$ : spheres, C: black circles): F - rotated ( $P\frac{6}{m}mm$ ), G - rotated plus shift ( $P\bar{6}2m$ ).

### III. RESULTS AND DISCUSSION

#### A. Geometries and total energies

##### 1. Cyanides MCN

The properties of the studied coinage metal cyanides CuCN, AgCN and AuCN are found to be very similar concerning geometries and total energies. Like in the case of AuCN,<sup>3</sup> our simulations reproduce, for the two other compounds, the experimentally known geometry within the chain and predict the possible existence of a sheet-type structure. The chain-type structure of AgCN and CuCN is known to differ from that of AuCN due to an even weaker chain-chain interaction. In the case of AuCN the aurophilic interaction keeps the interchain structure to a large extent ordered (6-fold  $P6mm$  symmetry about the chain axis), whereas in the former cases there is a considerable degree of disorder, leading to a lower 3-fold symmetry.<sup>5,6,7</sup> For the present analysis all the chain-type structures were confined to the  $P6mm$  symmetry (Fig. 1: A'). This is well sufficient for the description of the strong covalent bonds C-N, M-C, and M-N within the chains. The interchain search geometry for CuCN and AgCN is not the one experimentally suggested but, as the attraction between the chains is due to dispersion, DFT-GGA is not expected to perform correctly for this distance in any case.

For the  $M_3C_3N_3$  sheet structures, a total energy minimum was found for the 'simple stacking' geometry (see Fig. 1: B'), with symmetry  $P\bar{6}2m$ , whereas no stable structures were found corresponding to the other sheet geometries. The total energies for the chain and sheet structures are compared in Table I. The energy differences are about 0.2 eV for CuCN and AgCN, but for AuCN there is practically no difference between the two structures. Due to the weak sheet-sheet and chain-chain interactions, the comparison of the isolated structures leads to the same conclusion.

Table II gives the bond lengths and the lattice constants, along with the experimental values for the known M-N, M-C and C-N distances. We compare our re-

TABLE I: Total energy difference  $\Delta E$  (eV) between the chain and sheet structures for Group 11 metal cyanides (per MCN formula unit). Both 3D and isolated cases are reported. Negative value indicates that the chain structure is more stable.

Case	CuCN	AgCN	AuCN
3D Sheet vs. 3D Chain	-0.22	-0.18	0.00
2D Sheet vs. 1D Chain	-0.24	-0.21	0.03

sults with the experimental values from Hibble and co-workers<sup>6,7,21</sup>, who performed a systematic total neutron diffraction study for these structures. Their results differ somewhat from the conventional Bragg scattering studies, which, according to them, do not yield completely satisfactory results. For the chain structures, the experimental intrachain covalent bond lengths are very well described with distances accurate to 2% or better. In particular, the C-N distance is well reproduced. The difference between the M-C and M-N bond lengths in sheets compared to the same difference in chains, is larger. For sheets, the C-N bond lengths are practically the same for all the cyanides, but larger by about 20 pm compared to the chain structure, reflecting the aromatic six-ring bonding, as contrasted to the  $-C\equiv N$ - triple bonds.

Because of the well known difficulties in describing dispersion effects by DFT, the interchain and intersheet distances should be considered much more uncertain, which can be seen in the large theory-experiment discrepancy of the lattice parameter  $a$  for AuCN, which for this system corresponds to the chain-chain distance. The comparison of the interchain distances with the experimental values is further complicated, because the chains are randomly displaced along the chain axis, and for AgCN and CuCN there are no chemical bonds between the chains<sup>6,7,21</sup>. As a matter of fact, the latter is reflected in the very weak binding energy between the isolated and packed CuCN and AgCN chains in our calculations. The binding energy for isolated sheets required to form a 3D structure is found to be typically 0.05 eV.

It is interesting to note that room-temperature powder-X-ray pattern for CuCN shows unexplained weak Bragg peaks at distances  $d_1 = 260.5$  pm and  $d_2 = 235.3$  pm (Ref.7). These have been attributed to an unknown highly crystalline form  $\beta$ -CuCN with density  $2.97$  g cm<sup>-3</sup> (cf.  $3.03$  g cm<sup>-3</sup> for the known  $\alpha$ -CuCN). Whether such peaks could be correlated with our predicted sheet-type geometry or its modifications remains an open question. The crystal density of the sheet structure is  $1.8$  g cm<sup>-3</sup>, i.e.,  $\sim 40\%$  smaller than that assigned to  $\beta$ -CuCN. This computed density is, however, strongly influenced by the sheet-sheet distance  $c$ , which is possibly underestimated due to the lack of dispersion interaction. The present value of  $c$  is  $\sim 28\%$  and  $\sim 41\%$  larger than the distances  $d_1$  and  $d_2$ , respectively.

## 2. Dicarbides $MC_2$

The geometries of the metal dicarbides in the known experimental chain structure ( $M = \text{Mg-Ba}$  in Group 2) are well reproduced by our calculations. In addition, also for the dicarbides we predict the possible existence of sheet structures for both Groups 2 and 12, and for Group 12 we find possible chain structures. Experimentally, the Group 2 dicarbides crystallize in two different tetragonal symmetries, *viz*  $I4/mmm$  for  $MC_2$  ( $M = \text{Ca-Ba}$ ) and  $I4_2/mnm$  for  $\text{MgC}_2$ . Table III contains the calculated bond lengths and lattice parameters for the Group 2 chain dicarbides in comparison with the available experimental data. Table IV contains the predictions for chain structures for the Group 12.

As most of the chain- and sheet-type dicarbide structures were found to have no or low imaginary frequencies, the structures can be considered stable. The frequencies are presented in Sec. III B. Notable exceptions are  $\text{BeC}_2$  and  $\text{Be}_3\text{C}_6$ , which exhibited imaginary frequencies of the order of  $300i \text{ cm}^{-1}$ , suggesting that the found minimum energy geometry is only a transition state between phases of other symmetry. We did not try to follow the mode to a lower-symmetry minimum. Some imaginary frequencies of the order of  $100i \text{ cm}^{-1}$ , were found for chain-type  $\text{MgC}_2$ , whose structure is, however, in a very good agreement with the experiment. Smaller imaginary frequencies (about  $50i \text{ cm}^{-1}$  or smaller) were found for  $\text{ZnC}_2$ ,  $\text{CdC}_2$ ,  $\text{Ca}_3\text{C}_6$ ,  $\text{Sr}_3\text{C}_6$  and  $\text{Ba}_3\text{C}_6$ . We believe the origin of these imaginary frequencies is related either to the numerical inaccuracies or the anharmonicity of the total energy surface. In fact, small imaginary frequencies have been interpreted in terms of soft mode phonons.<sup>22</sup>

For the known Group 2 dicarbides in the chain structure, the calculated covalent bond lengths are in good agreement with experiment. Our calculations systematically give slightly larger values of the C-C bond length (around 125 pm) compared to the experimental results (around 120 pm), the C-C bond length in acetylene molecule<sup>23</sup> (120.4 pm) or the bond length calculated from the carbon triple-bond covalent radius (120 pm)<sup>24</sup>. A possible reason for the difference could be the vibrational motion of the dicarbide group in the experiments<sup>9</sup>. In realistic physical conditions, when thermal energy is applied,  $\text{C}_2^{2-}$  group can both rotate and vibrate, thus leading to an underestimation of the C-C bond length by experimental measurement. An interesting point to notice is that for  $\text{ZnC}_2$ ,  $\text{CdC}_2$  and  $\text{HgC}_2$ , we predict the possible existence of a chain structure in the  $I4/mmm$  geometry similar to the  $MC_2$  ( $M = \text{Ca-Ba}$ ) structures. The  $I4_2/mnm$  geometry for  $\text{ZnC}_2$ ,  $\text{CdC}_2$  and  $\text{HgC}_2$  was also found to be stable, but with slightly higher energies.

The difference in the packing geometry of the chain-type dicarbides compared to the packing geometry of the coinage metal cyanides can be understood from the different relative contributions to the interaction forces. Between the monovalent  $(\text{Au}^+)(\text{CN}^-)$  chains the dispersion forces predominate and one  $\text{Au}^+$  is surrounded by six

other nominally  $\text{Au}^+$  ions. For the divalent  $(M^{2+})(\text{C}_2^{2-})$  chains, on the other hand, the Coulomb forces predominate. Hence in this case the  $(M^{2+})(\text{C}_2^{2-})$  chains are displaced with respect to each other, so that one  $M^{2+}$  ion is surrounded by four  $\text{C}_2^{2-}$  ions (see Fig. 2: B, C). In support of this, infinite  $(M^{2+})(\text{C}_2^{2-})$  chains packed into a tetragonal  $P4mm$  unit cell (see Fig. 2: A) were found purely repulsive.

In the search of stable 2D infinite metal dicarbide sheets  $M_3C_6$ , the similar hexagonal symmetry D as in the  $M_3C_3N_3$  systems B' was used as a starting point (initially with a large sheet separation). Here, the benzene-like carbon rings are coupled together from the corners by the metal atoms. The calculations in this geometry yielded minimum energy structures for  $M = \text{Be, Zn-Hg}$ . For the remaining metals, the isolated 2D sheet spontaneously relaxed to a slightly different geometry within the same hexagonal crystal symmetry. The carbon rings rotated  $30^\circ$  with respect to the initial structure to yield the 2D sheet geometry shown in F and G. In this structure the metal atoms are located in the midpoint of the line connecting the C-C edges of every two benzene-like rings. Considering the 3D stacking of these structures, a 'simple stacking' (both 'rotated' and 'nonrotated' cases) was found purely repulsive. Instead, a new 3D packing had to be introduced, where every second sheet was translated by the vector  $\vec{v} = (\frac{1}{2}a, \frac{1}{2}a, 0)$ . For both the structures (E and H), stable geometries were found.

Fig. 5 summarizes the behavior of total energies for the most stable sheets and chains (the numerical values are tabulated later on in Sec. III D). The energy difference  $\Delta E$  is given for each dicarbide per  $MC_2$  unit; a negative value indicates that the chain structure is preferred. For the experimentally known dicarbides,  $M = \text{Mg-Ba}$ , the chains are energetically more stable. The energy difference roughly increases following  $Z$ , being in all the cases less than 1 eV. Interestingly, for the dicarbides not experimentally known,  $M = \text{Be, Zn, Cd}$  and  $\text{Hg}$ , the sheet structure is predicted to be the most stable phase, and the energy difference likewise increases roughly following  $Z$ .

## B. Vibrational frequencies

For the cyanide structures, vibrational analysis was performed for isolated chains and isolated sheets, whereas for dicarbides the analysis was done for packed chains and isolated sheets. The rest of the packed structures were not studied because of the difficulties due to the weak chain-chain (for cyanides) and sheet-sheet (for both cyanides and dicarbides) interactions. The frequencies are given in Figs. 6-8, and Tables VI and VII, VIII with comparison to available experiments.<sup>5,9,10,11,25</sup>

Following the assignment by Bowmaker *et al.*<sup>5</sup> for the modes in infinite cyanide chains, it can be seen that the simulation reproduces very well both the vibrational and bending normal modes for the known structures. Here

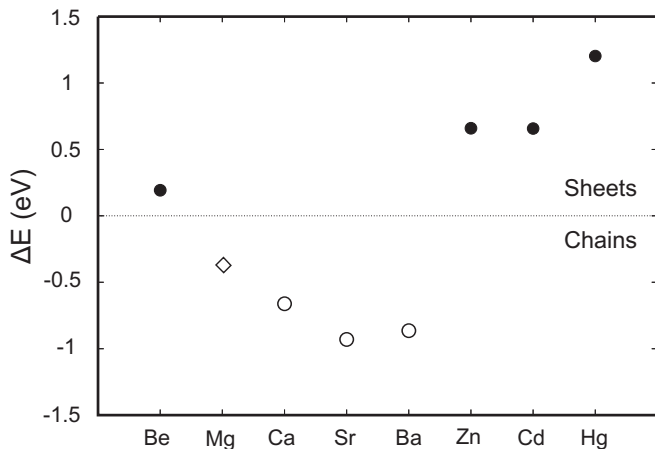


FIG. 5: Total energy differences (eV) between the most stable chain and sheet structures for Group 2 and 12 metal dicarbides: Chain B - Sheet F (●); Chain B - Sheet H (○); Chain C - Sheet F (◇).

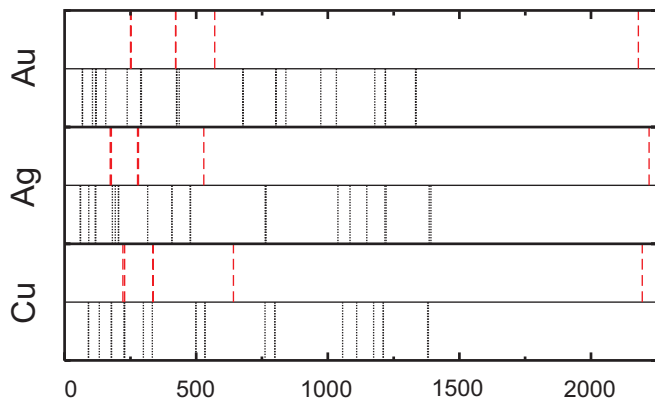


FIG. 6: Calculated vibrational frequencies ( $\text{cm}^{-1}$ ) for Group 11 metal cyanides. Dotted lines (black) refer to the sheet-type structures, dashed lines (red) refer to the chain-type structures. For comparison with experiment, see Table VI.

the two highest modes are the  $\nu(\text{CN})$  and  $\nu(\text{MC/N})$  stretching modes, and the two lowest ones the  $\delta(\text{MCN})$  and  $\delta(\text{NMC})$  bending modes. For the known dicarbides in the chain structure, the highest frequencies correspond to the stretching mode and are very close to the experimental ones.

The sheet structures for both cyanides and dicarbides exhibit systematically smaller maximum frequencies compared to those of the chain structures. The higher eigenfrequencies for sheets correspond to in-plane vibrations. Similarly as the bending modes in chains, the majority of the lower frequencies in sheets corresponds to bending vibrations perpendicular to the plane. For AuCN, the first and second frequency (Table VI) are close to the in-plane ring deformations of an isolated molecule ( $1395$  and  $1208\text{cm}^{-1}$ ) (Ref. 3).

We propose that the possible experimental identification of the sheet-type structures for cyanides could be performed within the range of roughly ( $650\text{-}1500$ )  $\text{cm}^{-1}$ .

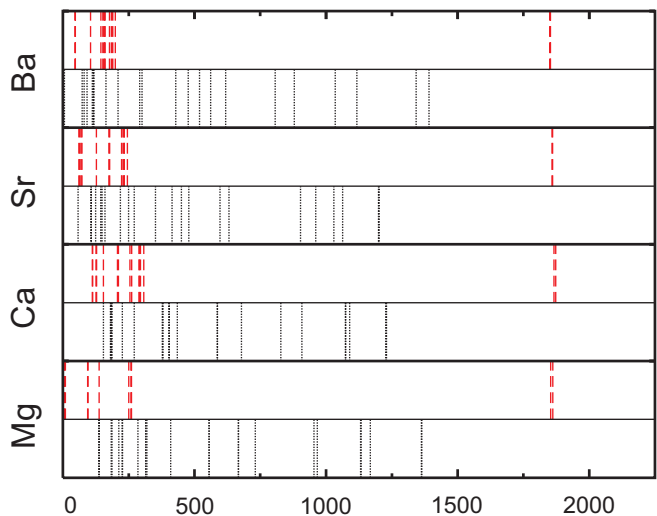


FIG. 7: Calculated vibrational frequencies ( $\text{cm}^{-1}$ ) for Group 2 metal dicarbides. Dotted lines (black) refer to the sheet-type structures, dashed lines (red) refer to the chain-type structures. For comparison with experiment, see Table VII.

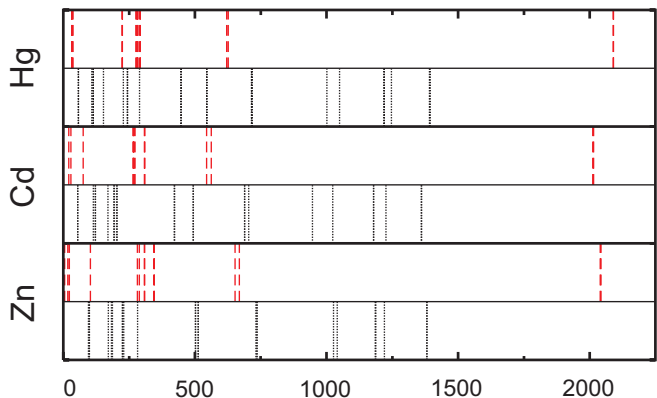


FIG. 8: Calculated vibrational frequencies ( $\text{cm}^{-1}$ ) for Group 12 dicarbides. Dotted lines (black) refer to the sheet-type structures, dashed lines (red) refer to the chain-type structures.

The majority of the in-plane vibrations of the sheets falls into this wavelength region, where no frequencies corresponding to chains interfere. Similarly, the identification of sheet-type dicarbides could be done in the range ( $700\text{-}1800$ )  $\text{cm}^{-1}$ , undisturbed by the frequencies of the known chain structures. The frequencies in these ranges correspond mainly to vibrations parallel to the sheets (i.e., parallel to the covalent bonds), and are thus not significantly affected by the DFT deficiencies for dispersion.

### C. Band gap and metallicity

The band gap values for the studied systems are reported in Table IX. Since a full band structure analysis was not performed, the values given should be considered as indicative only. In the case of both cyanide and dicar-

bide chain structures, all the known and predicted 1D (isolated) and 3D structures are found to be insulators. For the packed 3D dicarbide chain structures, the band gap is largest for  $\text{HgC}_2$  (3.7 eV) and smallest for  $\text{BaC}_2$  (1.6 eV). The packed chain structures exhibit systematically smaller band gaps than the isolated chains due to the increased overlap of the valence orbitals. The only exception to this picture is  $\text{BaC}_2$ , which seems to show an opposite trend. All the newly predicted chain dicarbides ( $M = \text{Zn-Hg}$ ) have larger gaps than the already known chain dicarbides.

For both cyanide and dicarbide 2D (isolated) and 3D sheet structures the band gaps are clearly smaller than for the chain structures. Packing the sheets to a 3D structure decreases, furthermore, very strongly the band gap value. For dicarbide sheets we identify two candidates that could be purely metallic compounds:  $\text{Sr}_3\text{C}_6$  and  $\text{Ba}_3\text{C}_6$ . Both systems may have a significant amount of charge carriers (we find this for both isolated and 3D sheet structures). The rest of the cyanide and dicarbide compounds are found to be either insulators or semimetals with a slight band overlap between the occupied and unoccupied states. In the 3D packed sheet geometry,  $\text{Zn}_3\text{C}_6$  and  $\text{Hg}_3\text{C}_6$  have the highest gaps ( $\sim 0.7$  eV).

#### D. Formation energy of dicarbides $M_3\text{C}_6$

We have estimated the formation energy of the predicted new dicarbides as the difference between their total energy and the total energy of the corresponding pure elemental metal and graphite:

$$E_F = E(MC_2) - [E(M) + 2E(C)], \quad (1)$$

where  $E(MC_2)$  is the total energy of the chain or sheet structure per  $MC_2$  unit.  $E(M)$  and  $E(C)$  are the total energies of one atom in the zero-temperature phase of the bulk crystal and in graphite, respectively. The total energy for graphite was calculated to be -9.18 eV. The results are given in Table X, where we have also given the atomization energies for the elemental metals, which compare reasonably well with experimental formation enthalpies.

From a thermodynamic consideration, we see that the formation of the dicarbides of Mg and Zn-Hg is clearly en-

dothermic, while  $\text{CaC}_2$ - $\text{BaC}_2$  are nearly thermoneutral. Of them, the  $MC_2$ ,  $M = \text{Mg, Ca, Sr and Ba}$ , exist. As check on the method, we compare the calculated atomization energies for the metals. Instead of graphite, which is a highly stable material, one could think of different benzene-derived substances as possible starting materials in the synthesis of the predicted new sheet-type compounds.

## IV. CONCLUSIONS

We have suggested a number of new solid substances, of which the sheet-type  $M_3\text{C}_3\text{N}_3$  ( $M = \text{Cu, Ag, Au}$ ) and the sheet-type  $M_3\text{C}_6$  ( $M = \text{Mg-Ba}$ ) may have the best chance of being prepared. The density of the new substances is in general lower than that of the known chain-type structures. For the identification of these new substances we have reported their vibrational frequencies. The majority of the in-plane frequencies of the new compounds are clearly separated from the stretching and bending frequencies of the known chain-type cyanide and dicarbide structures. Evidence is found that the Sr and Ba sheet-type compounds could be metallic both in the 3D crystal and as isolated sheets. All the Group 2 or Group 12 sheet-type structures are endothermic. The least endothermic one is calcium carbide. If any of these compounds can be made, the metallic Sr and Ba ones may find the most interesting applications. The sheet structures of lanthanides might form a further possible class of new compounds. Note that  $\text{CaC}_2$ -structured, insulating or metallic  $LnC_2$  are known for  $Ln = \text{Y, La, Ce, Tb, Yb, Lu and U}$ .<sup>28</sup>

#### Acknowledgments

We belong to the Finnish Center of Excellence in Computational Molecular Science (2006-2011). The grants 110571, 200903, 201291, 205967 and 206102 of The Academy of Finland are also gratefully acknowledged. The work was also supported by the Research Funds of the University of Helsinki.

<sup>1</sup> L. Gagliardi, *Theor. Chem. Acc.* **116**, 307 (2006).

<sup>2</sup> G. S. Zhdanov and E. A. Shugam, *Zh. Fiz. Khim.* **19**, 519 (1945).

<sup>3</sup> M. O. Hakala and P. Pyykkö, *Chem. Comm.* 2890–2892 (2006).

<sup>4</sup> M. I. Katsnelson, K. S. Novoselov, and A. K. Geim, *Nature Physics* **2**, 620 (2006).

<sup>5</sup> G. A. Bowmaker, B. J. Kennedy, and J. C. Reid, *Inorg. Chem.* **37**, 3968 (1998).

<sup>6</sup> S. J. Hibble, S. M. Cheyne, A. C. Hannon, and S. G. Eversfield, *Inorg.Chem.* **41**, 1042 (2002).

<sup>7</sup> S. J. Hibble, S. M. Cheyne, A. C. Hannon, and S. G. Eversfield, *Theor. Chem. Acc.* **41**, 4990 (2002).

<sup>8</sup> R. W. Henn, C. Bernhard, R. K. Kremer, T. Gulden, A. Simon, T. Blasius, and C. Niedermayer, *Phys. Rev. B* **62** (2000).

<sup>9</sup> P. Karen, A. Kjekshus, Q. Huang, and V. L. Karen, *J. Alloys and Compounds* **282**, 72 (1999).

- <sup>10</sup> V. Vohn, M. Knapp, and U. Ruschewitz, *J. Solid State Chem.* **151**, 111 (2000).
- <sup>11</sup> V. Vohn, W. Kockelmann, and U. Ruschewitz, *J. Alloys and Compounds* **284**, 132 (1999).
- <sup>12</sup> G. Kresse and J. Hafner, *Phys. Rev. B* **47**, 558 (1993).
- <sup>13</sup> G. Kresse and J. Furthmüller, *Comput. Mater. Sci.* **6**, 15 (1996).
- <sup>14</sup> G. Kresse and J. Furthmüller, *Phys. Rev. B* **54**, 11169 (1996).
- <sup>15</sup> D. Vanderbilt, *Phys. Rev. B* **41**, 7892 (1990).
- <sup>16</sup> G. Kresse and J. Hafner, *J. Phys.: Condens. Matter* **6**, 8245 (1994).
- <sup>17</sup> P. E. Blöchl, *Phys. Rev. B* **50**, 17953 (1994).
- <sup>18</sup> G. Kresse and J. Joubert, *Phys. Rev. B* **59**, 1758 (1999).
- <sup>19</sup> J. Paier, R. Hirschl, M. Marsam, and G. Kresse, *J. Chem. Phys.* **122**, 234102 (2005).
- <sup>20</sup> J. P. Pedrew, K. Burke, and M. Ernzerhof, *Phys. Rev. Lett.* **77**, 3865 (1996).
- <sup>21</sup> S. J. Hibble, A. C. Hannon, and S. M. Cheyne, *Inorg. Chem.* **42**, 4724 (2003).
- <sup>22</sup> M. Sternik and K. Parlinski, *J. Chem. Phys.* **122**, 064707 (2005).
- <sup>23</sup> G. Herzberg and J. W. T. Spinks, *Z. Physik* **91**, 386 (1934).
- <sup>24</sup> P. Pyykkö, S. Riedel, and M. Patzschke, *Chem. Eur. J.* **11**, 3511 (2005).
- <sup>25</sup> M. Knapp and U. Ruschewitz, *Chem. Eur. J.* **7**, 874 (2001).
- <sup>26</sup> O. Reckweg, A. Baumann, H. A. Mayer, J. Glaser, and H.-J. Meyer, *Z. Anorg. Allg. Chem.* **625**, 1686 (1999).
- <sup>27</sup> D. R. Lide, *CRC Handbook of Chemistry and Physics* (1999).
- <sup>28</sup> M. Atoji, *J. Chem. Phys.* **35**, 1950 (1961).
- <sup>29</sup> To whom correspondence should be addressed. E-mail: Pekka.Pyykko@helsinki.fi

TABLE II: Bond lengths, lattice parameters  $a$  and  $c$  (pm) and volumes  $V$  ( $\text{\AA}^3$ ) for Group 11 metal cyanides. The volume is given with respect to one  $MCN$  unit. The values  $a$  and  $V$  given in italics are not directly comparable to the experiment due to the different crystal symmetry in the calculation. The capital letter after the compound refers to the crystal structures in Fig. 1.

Chains	Source	$M$ -C	$M$ -N	C-N	$a$	$c$	$V$
CuCN (A')	Calc.	182.0	181.9	117.4	<i>407.7</i>	481.2	<i>69.27</i>
	Exp. <sup>a</sup>	184.6	184.6	117.0	591.2(3)	486.107(3)	49.0467
AgCN (A')	Calc.	201.9	204.0	117.0	<i>410.8</i>	523.9	<i>76.56</i>
	Exp. <sup>b</sup>	206	206	116	590.32	528.29	53.1443
AuCN (A')	Calc.	194.3	198.3	116.8	379.4	511.3	63.74
	Exp. <sup>c</sup>	197.03(5)	197.03(5)	114.99(2)	340.5(4)	509.2(2)	51.1273
Sheet	Source	$M$ -C	$M$ -N	C-N	$a$	$c$	$V$
Cu <sub>3</sub> C <sub>3</sub> N <sub>3</sub> (B')	Calc.	187.6	190.0	136.6	650.7	332.4	81.24
Ag <sub>3</sub> C <sub>3</sub> N <sub>3</sub> (B')	Calc.	207.4	213.8	136.1	693.3	341.5	94.78
Au <sub>3</sub> C <sub>3</sub> N <sub>3</sub> (B')	Calc.	199.5	210.4	136.3	682.5	352.4	94.78

<sup>a</sup>Ref. 7

<sup>b</sup>Ref. 6

<sup>c</sup>Ref. 21

TABLE III: Experimental and calculated lattice parameters  $a$  and  $c$  (pm), cell volumes  $V$  ( $\text{\AA}^3$ ), symmetries and bond lengths (pm) for Group 2 metal dicarbides in the chain structure. Volume is given with respect to one  $MC_2$  unit. The capital letter after the compound refers to the crystal structures in Fig. 2.

Case	BeC <sub>2</sub> (B)		MgC <sub>2</sub> (C)		CaC <sub>2</sub> (B)		SrC <sub>2</sub> (B)		BaC <sub>2</sub> (B)	
	Calc.	Calc.	Exp. <sup>a</sup>	Calc.	Exp. <sup>b</sup>	Calc.	Exp. <sup>c</sup>	Calc.	Exp. <sup>d</sup>	
Lattice const.: $a$	390.6	396.9	393.42(7) <sup>a</sup>	391.3	388.582(4) <sup>a</sup>	414.4	411.43(2) <sup>a</sup>	440.6	439.43(6) <sup>a</sup>	
$c$	463.2	492.5	502.1(1)	640.0	640.05(1)	681.8	676.60(4)	724.1	712.5(2)	
Volume $V$	35.01	38.8	38.85	49.0	48.20	58.60	57.26	70.3	68.88	
Symmetry	I4/mmm	I4 <sub>2</sub> /mmm		I4/mmm		I4/mmm		I4/mmm		
Bond lengths										
Chain-chain dist.	276.1	280.6	278.2	276.7	274.7	293.0	290.8	311.6	310.7	
$M$ -C	169.1	217.8	217.4	256.8	255.5(4)	277.7	278.5(8)	298.8	297.0(7)	
C-C	124.9	125.8	121.5	126.4	129.7(8)	126.4	120(2)	126.6	118.6(13)	

<sup>a</sup>Ref.<sup>9</sup>

<sup>b</sup>Ref.<sup>25</sup>

<sup>c</sup>Ref.<sup>10</sup>

<sup>d</sup>Ref.<sup>11</sup>

TABLE IV: Calculated lattice parameters  $a$  and  $c$  (pm), cell volumes  $V$  ( $\text{\AA}^3$ ), symmetries and bond lengths (pm) for Group 12 metal dicarbides in the chain structure. Volume is given with respect to one  $MC_2$  unit. The capital letter after the compound refers to the crystal structures in Fig. 2.

Case	ZnC <sub>2</sub> (B)	CdC <sub>2</sub> (B)	HgC <sub>2</sub> (B)
Lattice constants: $a$	425.1	438.1	510.5
$c$	505.2	546.9	529.0
Volume $V$	45.7	52.5	68.9
Symmetry	I4/mmm	I4/mmm	I4/mmm
Bond lengths			
Chain-chain dist.	300.6	309.8	361.0
$M$ -C	190.5	211.2	202.9
C-C	124.2	124.5	123.2

TABLE V: Calculated lattice parameters  $a$  and  $c$  (pm), volumes  $V$  ( $\text{\AA}^3$ ), symmetries and bond lengths (pm) for Group 2 and 12 metal dicarbides in the sheet structure. Volume is given with respect to one  $MC_2$  unit. The capital letter after the compound refers to the crystal structures in Figs. 3-4.

Case	Be <sub>3</sub> C <sub>6</sub> (E)	Mg <sub>3</sub> C <sub>6</sub> (G)	Ca <sub>3</sub> C <sub>6</sub> (G)	Sr <sub>3</sub> C <sub>6</sub> (G)	Ba <sub>3</sub> C <sub>6</sub> (G)	Zn <sub>3</sub> C <sub>6</sub> (E)	Cd <sub>3</sub> C <sub>6</sub> (E)	Hg <sub>3</sub> C <sub>6</sub> (E)
Lattice const.: $a$	390.6	665.0	736.2	782.7	826.2	674.4	715.2	708.2
$c$	463.2	526.8	543.3	570.0	592.1	711.1	695.1	794.1
Volume $V$	56.9	67.2	84.9	100.7	116.9	93.4	102.6	115.1
Symmetry	$P\bar{6}2m$	$P\frac{6}{m}mm$	$P\frac{6}{m}mm$	$P\frac{6}{m}mm$	$P\frac{6}{m}mm$	$P\bar{6}2m$	$P\bar{6}2m$	$P\bar{6}2m$
Bond lengths								
$M-C$	168.9	214.2	246.2	273.2	280.4	194.8	214.9	212.7
$C-C$	142.9	142.9	143.2	140.0	141.2	142.6	141.9	140.7

TABLE VI: Experimental and calculated vibrational frequencies ( $\text{cm}^{-1}$ ) for Group 11 metal cyanides. For sheets, the four highest frequencies, which correspond to in-plane stretching modes, are reported. The close-lying frequencies have been grouped together.

Case	CuCN		AgCN		AuCN	
	Calc.	Exp. <sup>a</sup>	Calc.	Exp. <sup>a</sup>	Calc.	Exp. <sup>a</sup>
Chains						
Stretch (C-N)	2195	2170	2221	2164	2180	2236
Stretch ( $M-CN$ )	642	591	529	480	571	598
Bend 1	337,336	326	281,277	272	422,421	358
Bend 2	228,221	168	178,173	112	253,251	224
Sheets	Calc.	Exp.	Calc.	Exp.	Calc.	Exp.
	1382,1379	-	1392,1386	-	1336,1334	-
	1212,1210	-	1221,1216	-	1219,1218	-
	1174,1109,1057	-	1174,1087,1039	-	1178,1032,973	-
	799,798	-	763,762	-	804,802	-

<sup>a</sup>Ref.<sup>5</sup>

TABLE VII: Experimental and calculated vibrational frequencies ( $\text{cm}^{-1}$ ) for Group 2 and 12 chain-type dicarbides. The highest frequencies, which correspond to stretching modes along the chains, are reported. The close-lying frequencies have been grouped together.

Chains	MgC <sub>2</sub>	CaC <sub>2</sub>	SrC <sub>2</sub>	BaC <sub>2</sub>	ZnC <sub>2</sub>	CdC <sub>2</sub>	HgC <sub>2</sub>
Experimental value <sup>a</sup>	-	1860	1850	1832	-	-	-
Calculated value	1861,1854 261,260	1872,1866 308,294	1861,1860 245,234	1853,1851 200,190	2043,2040 669,652	2015,2012 563,545	2090,2090 627,621

<sup>a</sup>Ref. 26

TABLE VIII: Calculated vibrational frequencies ( $\text{cm}^{-1}$ ) for Group 2 and 12 sheet-type dicarbides. Only the highest frequencies values, which correspond to in-plane stretching modes, are reported. The close-lying frequencies have been grouped together.

Mg <sub>3</sub> C <sub>6</sub>	Ca <sub>3</sub> C <sub>6</sub>	Sr <sub>3</sub> C <sub>6</sub>	Ba <sub>3</sub> C <sub>6</sub>	Zn <sub>3</sub> C <sub>6</sub>	Cd <sub>3</sub> C <sub>6</sub>	Hg <sub>3</sub> C <sub>6</sub>
1364,1362	1230,1227	1202,1199	1391,1342	1382,1381	1361,1360	1394,1391
1168	1090,1074	1063,1030	1117,1035	1220	1226	1246
1134,1131	1073	963,901	879,807	1187,1185	1179,1178	1219,1218
966,954	909,828	631	619	1040,1027	1024,947	1050,1001

TABLE IX: HOMO/LUMO band gap (eV) for isolated and packed cyanide and dicarbide structures. The metallic or semimetallic character is indicated when relevant.

Case	Chains		Sheets	
	Isolated	Packed	Isolated	Packed
CuCN	3.9	2.5	1.6	0.2
AgCN	4.7	3.1	1.8	0.3
AuCN	4.6	2.3	1.6	0.2
BeC <sub>2</sub>	3.6	2.9	0.6	SM <sup>a</sup>
MgC <sub>2</sub>	4.2	2.0	1.5	SM
CaC <sub>2</sub>	2.6	1.7	SM	SM
SrC <sub>2</sub>	2.0	1.7	M <sup>b</sup>	M
BaC <sub>2</sub>	1.3	1.6	M	M
ZnC <sub>2</sub>	3.9	2.4	1.2	0.7
CdC <sub>2</sub>	4.0	2.8	0.6	SM
HgC <sub>2</sub>	3.8	3.7	0.9	0.7

<sup>a</sup>Semimetallic

<sup>b</sup>Metallic

TABLE X: Formation energy  $E_f$  for Group 2 and 12 sheet-type dicarbides and difference to the chains ( $\Delta E = E^{\text{chain}} - E^{\text{sheet}}$ ) per  $MC_2$  unit. The calculated atomization energy  $E_{\text{at}}^M$  and the experimental atomization enthalpy  $H_{\text{at}}^M$  for the pure element  $M$  are also given. All values are in eV.

Case	$E_f^{\text{sheet}}$	$\Delta E$	$E_{\text{at}}^M$	$H_{\text{at}}^M$ (exp. <sup>a</sup> )
Mg <sub>3</sub> C <sub>6</sub>	1.55	-0.36	1.51	1.531
Ca <sub>3</sub> C <sub>6</sub>	0.61	-0.65	1.91	1.847
Sr <sub>3</sub> C <sub>6</sub>	0.92	-0.91	1.61	1.704
Ba <sub>3</sub> C <sub>6</sub>	1.05	-0.85	1.88	1.866
Zn <sub>3</sub> C <sub>6</sub>	1.99	0.67	1.11	1.355
Cd <sub>3</sub> C <sub>6</sub>	2.32	0.65	0.72	1.161
Hg <sub>3</sub> C <sub>6</sub>	1.99	1.21	0.08	0.635

<sup>a</sup>Ref. 27